Phase-Separated Structures in Polymer Mixtures with a Thermotropic Liquid Crystalline Copolyester as One Component: Composition Dependence

Akemi Nakai,[†] Wei Wang,[‡] Shigeru Ogasawara,[§] Hirokazu Hasegawa, and Takeji Hashimoto*

Department of Polymer Chemistry, Graduate School of Engineering, Kyoto University, Kyoto 606-8501, Japan

Received January 21, 1998; Revised Manuscript Received June 8, 1998

ABSTRACT: The composition dependence of the phase-separated structures in the polymer mixtures consisting of a thermotropic liquid crystalline (LC) copolyester (X-7G) and poly(ethylene terephthalate) (PET) was investigated by means of polarized light microscopy. For this purpose the mixtures were solution-cast into thin films, followed by isothermal annealing at 270 °C. Although the final structure was the LC droplets dispersed in the isotropic matrix for all mixtures, a variety of pattern-forming processes were observed, depending on the composition. For the mixtures with higher X-7G content, dewetting of the X-7G component on the surface of the glass substrate played an important role in the pattern formation.

1. Introduction

Blending a high-performance liquid crystalline polymer (LCP) with a conventional plastics is an attractive route to create a novel high-performance plastics.[1,2] Interesting concepts such as self-reinforcing composites and molecular composites have been developed to describe immiscible and miscible polymer mixtures containing LCP.[2−12] However, it is disappointing that the mechanical properties of such mixtures are usually not as good as expected.[8−12] This is mainly due to the undesirable macroscopic phase separation of the mixtures. Many observations of the morphology of the mixtures obviously showed large LCP domains embedded in the isotropic matrix of the conventional plastics and distinct interfaces between the two phases.[8−12] This indicates the inherent immiscibility of the LCP with the conventional plastics and the lack of interfacial adhesion between the isotropic and anisotropic phases.

To achieve the optimum properties of LCP/conventional plastics blends, it is necessary to control both of the phase-separated structures and the interfacial structures. Therefore, basic researches on the mechanisms and the dynamics of the phase separation and interfacial properties of LCP/conventional plastics blends become very important. The major factors controlling the phase-separation of immiscible polymer mixtures are temperature, composition, and molecular characteristics of each component. Therefore, it is significant to study the effects of these factors on the phase-separation processes of the polymer mixtures containing LCP.

In our previous studies, we investigated the two-phase structures formed during phase separation[13] in the polymer mixture of a thermotropic liquid-crystalline copolyester (X-7G) and a conventional polyester (PET) with a fixed composition of 50/50 (wt %/wt %) as well as the mechanism and process of its phase separation.[14] We observed that the two-phase structures of the mixtures formed by phase separation were very sensitive to the test temperature. The vitrification and crystallization of the components at different stages of the phase separation could hinder the structures from their further growth. When the test temperature was higher than both of the melting points of the two components, the phase separation via spinodal decomposition (SD) occurred rapidly without pinning. In such cases, however, we could observe only the late stage SD (coarsening process) but not the early and intermediate stages in the time range of our investigation.[14] This may be attributed to the extremely rapid phase separation due to the high segregation power between the two components and the high mobility of the LCP molecules.

In this study, we extended our study to explore the composition dependencies of the phase-separated structures and phase-separation processes for the mixtures of X-7G/PET. We used the same polymer samples as those used in the previous studies.[13,14] Since the coarsening process was able to be observed for the 50/50 mixture of X-7G/PET only at temperatures higher than 270 °C (the melting point of the PET component),[13,14] we selected 270 °C as the unique test temperature in this experiment in order to observe time evolution of the phase-separated structures without influence of the solidifications due to vitrification and/or the crystallization. The effect of transesterification was also proved to be negligible under this experimental condition.[14] The observation was again performed in real space under a polarized light microscope. First, we present the composition dependence of the two-phase structures and the ordering processes. Then, we discuss

* To whom correspondence should be addressed.
[†] Present address: Department of Home Economics, Kyushu, Women's Junior College, 1-1 Jiyugaoka, Yawatanishi, Kitakyushu, 807, Japan.
[‡] Present address: Institute of Materials Research and Engineering, National University of Singapore, 10 Kent Ridge Crescent, Singapore 119260.
[§] Present address: CAE Technology Laboratory, Kyoto Technology Center, R&D Headquarters, Sekisui Chemical Co., LTD, Kamichoshicho 2-2, Kamitoba, Minami-ku, Kyoto 601, Japan.

S0024-9297(98)00070-9 CCC: $15.00
Published on Web 07/24/1998

the mechanisms of the structural growth in the mixtures with different compositions.

2. Experimental Section

A liquid crystalline copolyester produced by Tennessee Eastman Co. Ltd. with the trade name of X-7G comprising 60 mol % *p*-oxybenzoate (OBA) unit and 40 mol % ethylene terephthalate (ET) unit was used as the LCP component. A commercial poly(ethylene terephthalate) (PET) provided by Toray Co. Ltd. was used as a conventional plastics component. The number-average molecular weights of these polymers were both ca. 2×10^4.

A. Sample Preparation. Mixtures of X-7G and PET with the mixing ratio of X-7G/PET varying from 70/30 to 20/80 (wt %/wt %) were dissolved in *o*-chlorophenol at 60 °C to form ca. 2 wt % solutions. As mentioned in our previous reports,[13,14] the solutions contained a very small amount of insoluble particles, which were probably composed of crystalline copolymers with much higher OBA content than average. These insoluble particles were carefully removed by filtration before casting. A few drops of the filtered solution were placed on a microscope cover glass, which was then put into a vacuum oven to evaporate the solvent quickly under reduced pressure at 60 °C. Most of the solvent seemed to evaporate within a few minutes, and the polymer mixture was solidified to form a clear film on the glass surface. The film specimen was further dried under vacuum for 3 h to remove the remaining solvent. The sample codes are hereafter designated by the X-7G/PET (wt %/wt %) ratio such as 40/60.

The important features of the test specimens of all mixtures thus prepared are the following: Their top sides are free and in contact with air, and their bottom sides are in contact with the glass substrates. The center parts of the as-prepared film specimens with a diameter of ca. 10 mm had an average thickness of ca. 10 μm and appeared transparent. They were optically isotropic and homogeneous under a polarized light microscope. This indicates that the homogeneous mixture of the two components in the solution was quickly solidified in the film without significant phase separation due to the rapid evaporation of the solvent under vacuum, although the two components are essentially immiscible in bulk. Therefore, the polymers in the as-prepared film samples were both in the amorphous glassy state and the two kinds of molecules were uniformly dispersed at a length scale larger than the resolution limit of an optical microscope.

B. Experimental Methods. Phase separation started when the temperature of the test specimen was quickly raised from room temperature to the test temperature (270 °C) by placing it onto a microscope heating stage (LINKAM Scientific Co. TH-600) controlled at the test temperature (*T*-jump process). The test samples reached the test temperature within a few seconds. The subsequent ordering process was tracked by real-time and in-situ observations under a polarized light microscope (PLM) (Nikon Optiphot-Pol XTP-11) with a roll-film camera. Some specimens were quenched from the test temperature to room temperature in order to fix the phase-separated structure and then investigated further by means of PLM.

C. Image Analysis and Determination of Characteristic Length. The details concerning the analysis of the PLM images of the phase-separated structures and the determination of their characteristic length have been described in the previous paper.[14] Here, we briefly mention only the principles. We first binarized the video-recorded PLM images consisting of bright areas of LC domains rich in X-7G and dark areas of isotropic domains rich in PET with respect to a carefully selected threshold value by using an image-analyzing system. Then we scanned the binarized images in the horizontal and vertical directions to measure the repeat distance Λ between neighboring bright (or dark) areas. Furthermore, the domain-spacing distribution function $P(\Lambda,t)$, which is the probability of occurrence of a domain spacing Λ in the horizontal and vertical scans at time t, was determined. And finally, the average characteristic length $\Lambda_m(t)$ at time t was determined by the following equation:

$$\Lambda_m(t) \equiv \int_0^\infty \Lambda P(\Lambda,t)\, d\Lambda / \int_0^\infty P(\Lambda,t)\, d\Lambda \qquad (1)$$

3. Results

The PLM micrographs in Figure 1 were obtained with crossed polarizers from the same area for each X-7G/PET mixture with six different compositions in the time interval from 10 to 1000 s after the temperature jump to 270 °C. Since the optically anisotropic area rich in X-7G component appears bright and the isotropic area rich in PET component appears dark, time evolution of the phase-separated structures can be seen with high contrast. A higher magnification of the micrographs was chosen in Figure 1a than in Figure 1b to show the details of the phase-separated structures.

For 30/70 and 40/60, bright droplets of the LC phase rich in X-7G already appeared in the dark matrix rich in PET component at time $t = 10$ s, as shown in Figure 1a. But, the droplet size did not increase further with time for both mixtures, indicating that the coarsening hardly occurred after $t = 10$ s. The average size of the LC droplets is ca. 1 μm for 30/70 and ca. 4 μm for 40/60.

For 45/55, as shown in the right column of Figure 1a, partly disrupted LC networks were seen at $t = 10$ s. These networks rapidly broke up into the fragments with irregular shapes, as shown in the micrograph taken at $t = 30$ s. Subsequently, the fragments rounded up to form much larger droplets than those observed for 30/70 and 40/60.

The pattern formation process observed for 50/50 shown in the left column of Figure 1b has already been investigated and reported in the previous papers.[13,14] The process was classified into three regimes, which were summarized as follows: In regime I ($t = 5-200$ s), an optically anisotropic network of the LC phase was formed by spinodal decomposition, followed by the self-similar growth of the network by two mechanisms, i.e., (i) vaporization and condensation of the isotropic component and (ii) partial disruption and thickening of the network, while keeping the fraction of both bright and dark area constant at 0.5. In regime II ($t = 200-600$ s), the network disrupted into the fragments and its global continuity was lost, followed by the shrinkage of the fragments into circular droplets. In regime III, the diffusion and coalescence of the droplets took place ($t > 600$ s). The micrographs taken at $t = 1000$ s and $t > 1000$ s (not shown here) exhibited an interesting phenomenon that many droplets with different sizes coming in contact with each other through the diffusion process did not coalesce into larger droplets immediately. This phenomenon implies that the coalescence process of the droplets in this system is much slower than their diffusion process.

For 60/40, the pattern formation process seems to be similar to that observed for 50/50. However, the following features should be noted: (i) most of the isotropic domains observed at $t = 10$ and 30 s for 60/40 had a shape of circular or elongated droplets rather than a branched shape observed for 50/50; (ii) the rate of coarsening of the LC network is faster for 60/40 than that for 50/50; (iii) the fragments of the disrupted LC network rounded up more slowly for 60/40 than 50/50, so at $t = 1000$ s some anisotropic droplets still had nonspherical shapes, as shown by the images in Figure 1b.

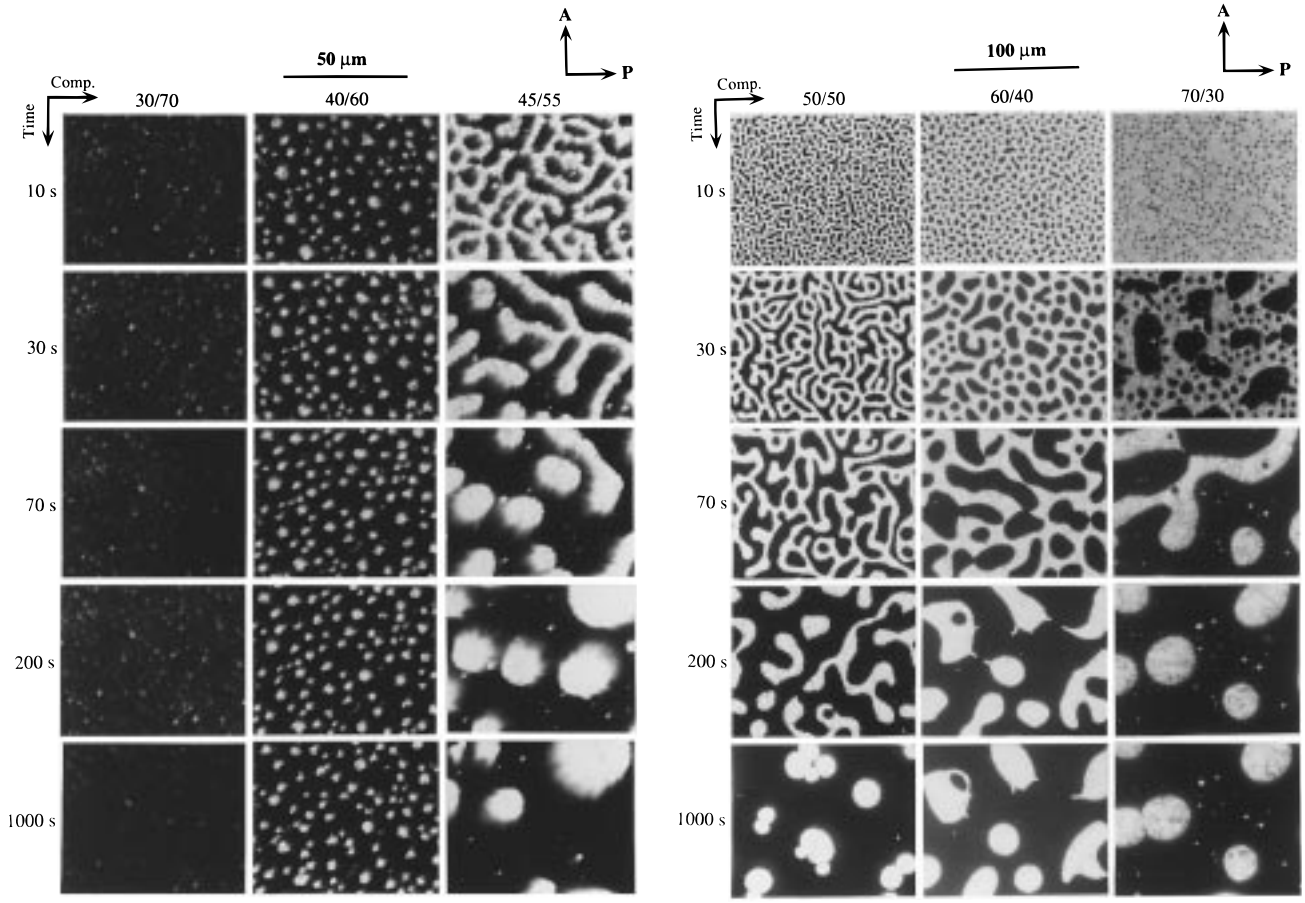

Figure 1. PLM micrographs of the film samples of the X-7G/PET mixtures showing the influence of the composition from 30/70 to 70/30 on the phase-separated structures at 270 °C for different annealing times. A and P designate the polarization directions of the analyzer and the polarizer. Bright areas are the optically anisotropic liquid-crystalline domains rich in X-7G, and dark areas are the optically isotropic melt rich in PET. (a, Left) the composition changes from 30/70 to 45/55 with a high magnification. (b, Right) the composition changes from 50/50 to 70/30 with a low magnification.

For 70/30, the pattern formation process was quite different from those of the other mixtures. A large number of small isotropic droplets were formed but their distribution in the LC matrix was not uniform (see the image obtained at $t = 10$ s). The rapid coalescence of the isotropic droplets resulted in the formation of a thick LC network which still contained small isotropic droplets inside. Therefore, two kinds of isotropic domains with quite different sizes coexist as shown by the image at $t = 30$ s in Figure 1b. In the following process, the small isotropic droplets were expelled from the LC network phase which simultaneously undergoes disruption. Finally, the LC fragments rounded up to form large LC droplets in the isotropic matrix like 45/55, 50/50, and 60/40.

Observation of these mixtures earlier than $t = 10$ s may be useful for further understanding the phase-separation process. Since an in-situ observation was quite difficult for such short time, we observed the quenched samples instead. Figure 2 shows the PLM micrographs of X-7G/PET mixtures with different compositions quenched after 3 s annealing at 270 °C. Because the thickness of the sample films was ca. 10 μm and the sizes of the phase-separated structures in Figure 2 are smaller than 10 μm, the structures have the three-dimensional characteristic to some extent. For 30/70, the optically anisotropic droplets with the diameter smaller than 3 μm had already formed by this time. For 40/60, however, partly disrupted networks of X-7G with a thickness of ca. 1−2 μm were seen. The LC network seems to have rapidly broken up and rounded up into droplets, as no LC network and fragments were observed at $t = 10$ s (see Figure 1a). For 50/50, a bicontinuous network structure composed of the LC and isotropic domains was observed. Note that Schlieren texture is seen in the LC network for 40/60 and 50/50. Although the network structure of the isotropic phase is difficult to see at a glance, modulation of the brightness of the LC phase suggests the overlapping of the LC and isotropic phases in the thickness direction. For 60/40 and 70/30, dark isotropic droplets of PET-rich domains were dispersed in the LC matrix with Schlieren texture. It is impressive to note that the interface of the isotropic droplets is not smooth but rather irregular, even appearing to have edges.

4. Discussion

A. Time Dependence of the Average Characteristic Length. In our previous study,[14] we found the coarsening process in 50/50 obeys power laws and a different power law holds for each regime of the coarsening process. Namely, the time dependence of the average characteristic length Λ_m is given by

$$\Lambda_m \sim t^{\alpha} \tag{2}$$

where α is $-1/3$, -1, and $-1/6$ for regimes I, II, and III, respectively. The coarsening eventually stops at a long time limit where α becomes 0.

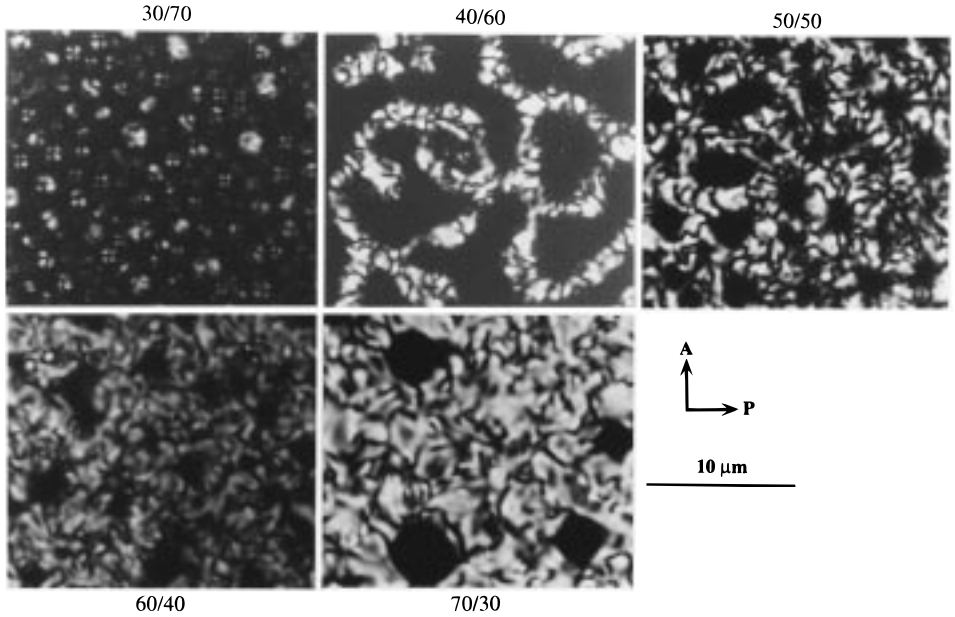

Figure 2. PLM micrographs of the quenched film samples of the X-7G/PET mixtures showing the composition dependence of the phase-separated structures at $t = 3$ s.

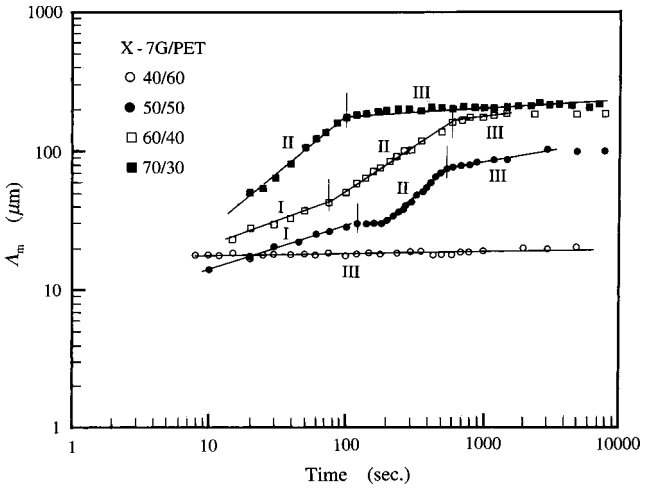

Figure 3. Double logarithmic plots of the average characteristic length Λ_m vs time t for the mixtures with the compositions as indicated in the figure. Three regimes, delimited according to the previously reported classification concepts for 50/50,[14] are indicated in the figure. In each regime, a linear relation between log Λ_m and log t is identified.

Figure 3 shows the double logarithmic plots of Λ_m vs time t obtained from the analyses of the PLM images during the phase-separation processes after the T-jumps to 270 °C for 40/60, 50/50, 60/40, and 70/30. For 60/40 and 70/30 in addition to 50/50, the coarsening processes seem to obey power laws. In general, Λ_m at a given t increases with increasing weight fraction of X-7G, probably due to the lower viscosity (higher mobility) of the LC domains. According to the classification of the phase-separation process of 50/50 into three time regimes (regimes I, II, and III) with different coarsening mechanisms, as reported in our previous paper[14] and briefly mentioned above, we delimited the regimes for 60/40 and 70/30 as shown in Figure 3. A linear relation between log Λ_m and log t was identified in each regime. The slopes α of the linear lines in each regime are pretty much the same for different compositions except for region II of 60/40, which gives a smaller α than 1. This is in accordance with the slower rounding-up process of the LC fragments for 60/40 as observed by the PLM images in Figure 1b.

The data for 30/70 were not plotted in Figure 3 because no coarsening was observed for this mixture and Λ_m remained at a few micrometers. Accurate determination of Λ_m was not easy because of the Schlieren textures in the LC droplets and the small droplet size as shown in the PLM image in Figure 2.

For 40/60, only the regime III was observed during annealing at 270 °C; namely, the mixture was composed of the LC droplets dispersed in the isotropic matrix in the time interval covered in this experiment, as shown in Figure 1, and Λ_m hardly increased with time. However, the PLM image of partly broken LC networks for the quenched sample at $t = 3$ s as shown in Figure 2 implies the existence of regime II at time shorter than 6 s and possibly the existence of regime I at time shorter than 3 s.

For 60/40, all three regimes were observed, indicating that the phase-separation process is similar to that for 50/50. For 70/30, only regimes II and III were observed in Figure 3. This, together with the PLM observation in Figure 1, indicates that the mechanism of phase separation at the initial stage for 70/30 is quite different from that for 50/50, which will be discussed later.

Figure 4 shows the average radius of the LC droplets at the longest annealing time for each composition, $\bar{R}$, as a function of weight fraction of the X-7G component, Φ_{X-7G}. ($\bar{R}$ was determined from the measurement over the area much larger than that shown in Figure 1.) In general, $\bar{R}$ increases with Φ_{X-7G} but the increase in $\bar{R}$ with Φ_{X-7G} is not monotonic. For $\Phi_{X-7G} \leq 0.3$ and $0.5 \leq \Phi_{X-7G}$, log $\bar{R}$ increases very slowly with Φ_{X-7G}, while for $0.3 \leq \Phi_{X-7G} \leq 0.5$, log $\bar{R}$ increases very rapidly with Φ_{X-7G}.

B. Domain-Growth Mechanism in 30/70 and 40/60. In 30/70 and 40/60, the phase-separated structure after $t = 10$ s is mainly composed of the LC droplets rich in X-7G dispersed in the isotropic matrix rich in PET, except for the very early stage of the 40/60 case. Since the diameter of the LC droplets is smaller than the thickness of the film specimen ($\sim 10\,\mu$m), the domain

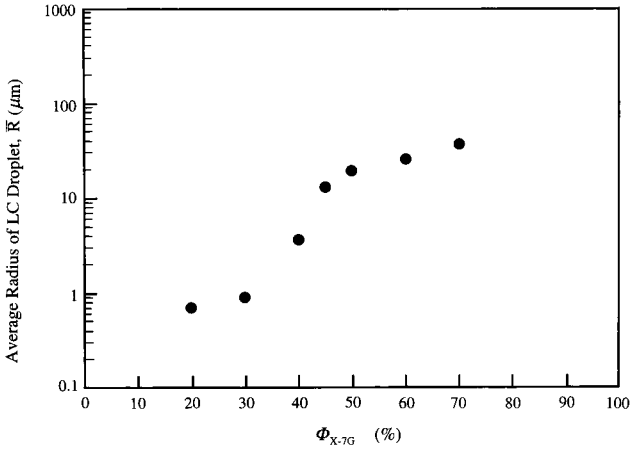

Figure 4. Average final size of the LC droplets, $\bar{R}$, plotted as a function of weight fraction of X-7G component, Φ_{X-7G}, with the semilogarithmic scale.

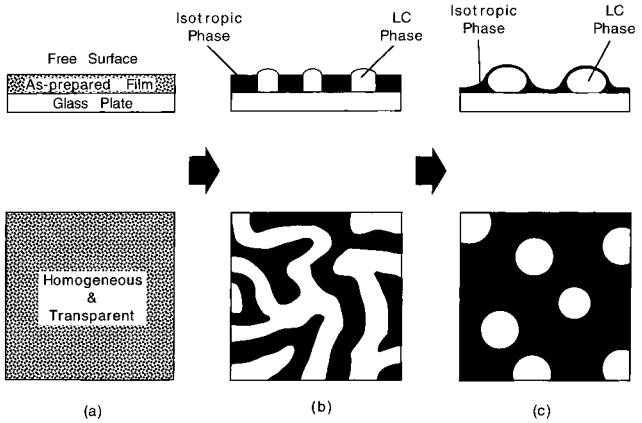

Figure 5. Schematic representation of the evolution of the phase-separated structure [(top) side views, (bottom) top views] in the three-dimensional space for the mixtures from 45/55 to 60/40. (a) as-prepared specimen; (b) regime II; (c) regime III.

growth should be three-dimensional. The translational diffusion and subsequent coalescence of small anisotropic droplets, which possibly leads to an increase in the droplets size, should be the dominant mechanism of the domain growth. However, the probability of the coalescence of droplets seems to be very low in this case, so the droplet size remains almost constant in the time interval covered in this observation (see Figure 3). Therefore, the final size $\bar{R}$ of anisotropic droplets is small (see Figure 4).

In Figure 2, most of the small LC droplets in the PLM image of 30/70 show the Schlieren texture with four dark brushes resembling the maltese cross in a spherulite. Such a pattern can be interpreted by the "radial" structure containing a point volume defect (hedgehog) in the bulk of the droplet; i.e., the directors of the LC molecules are aligned along the radial directions of the spherical droplets surrounded by the isotropic matrix, as reported for *N*-(4-methoxybenzylidene)-4-butylaniline (MBBA) LC droplets suspended in an isotropic poly(dimethylsiloxane) matrix.[15] Much larger LC droplets observed in the mixtures with other compositions do not exhibit such a simple texture, because of their oblate-spherical shape with the diameters exceeding the film thickness and because of many disclinations within them.

C. Domain-Growth Mechanism in 45/55, 50/50, and 60/40. The domain-growth mechanisms in 45/55, 50/50, and 60/40 are similar to each other. Since we discussed the domain-growth mechanism for 50/50 in detail in our previous paper,[14] we briefly mention it here. For 50/50, the area fraction of isotropic phase, ϕ_I, evaluated from the PLM images remained constant at 0.5 in regime I but rapidly increased to more than 0.7 in regime II and approached a constant value of 0.83 in regime III. This suggests that the disruption of the LC network and the following rounding up of the LC fragments in regime II are accompanied by the protruding of the LC domains, while the film surface is kept essentially flat during the self-similar growth of the LC percolation network in regime I. This is considered as a dewetting phenomenon and the process is schematically illustrated in Figure 5.

Figure 5a shows the as-cast film of the homogeneous mixture on the glass plate. The film surface is flat. In regime I, as soon as the phase separation starts, the percolation network structure of the LC phase is formed, followed by the self-similar growth of the percolation network structure as often observed for the late stage spinodal decomposition. When the thickness of the LC network becomes comparable to that of the film specimen, the structural growth turns from three-dimensional to two-dimensional. The situation at this moment is illustrated in Figure 5b. Since the interfacial tension between the LC phase and the glass is much larger than that between the isotropic phase and the glass, the LC phase tends to minimize the area in contact with the glass surface by pushing up the free surface and expanding itself normal to the film surface. However, because the percolation network structure tends to keep the thickness of the film constant, roughening of the surface does not become so significant yet. In regime II, finally this balance is lost, the LC network rapidly breaks up into fragments, and the LC fragments rapidly degenerate into the droplets protruding from the isotropic matrix, as illustrated in Figure 5c, due to dewetting against the glass surface and also due to losing the network structure. This leads to the rapid growth of both Λ_m and ϕ_I. In Figure 3, we can see that the breakup of the LC network occurs at a critical value of $\Lambda_m \approx 30$ μm for 50/50; i.e., the domain size (ca. 15 μm) is slightly larger than the film thickness (ca. 10 μm).

Thus, the percolation-cluster transition observed for 45/55, 50/50, and 60/40 is not the kind observed for spinodal decomposition of off-critical mixtures, but it is a result of dewetting phenomena. On the other hand, the percolation-cluster transition observed for 40/60 between $t = 3$ and 10 s may be considered as the former.

In regime III, the phase-separated structure is composed of the LC droplets dispersed on/in the isotropic matrix, as schematically shown in Figure 5c, so the ordering mechanism is the diffusion-coalescence of droplets.[16] At the early stage of regime III, log Λ_m increased slowly with time (Figure 3) and showed a scaling relation of $\Lambda_m \sim t^{1/6}$. At the late stage of regime III, the growth of log Λ_m stopped and $\Lambda_m \sim t^0$, showing cessation of the droplet movement.

D. Domain-Growth Mechanism in 70/30. To investigate the domain-growth mechanism in the 70/30 mixture, the time evolution of the PLM images is shown more in detail in Figure 6. The coarsening process was divided into three time regimes according to the classification of 50/50.[14] Regimes II and III shown in Figure 6 are very similar to those of 50/50,[14] but "regime I" is quite different. In "regime I" of 70/30, a

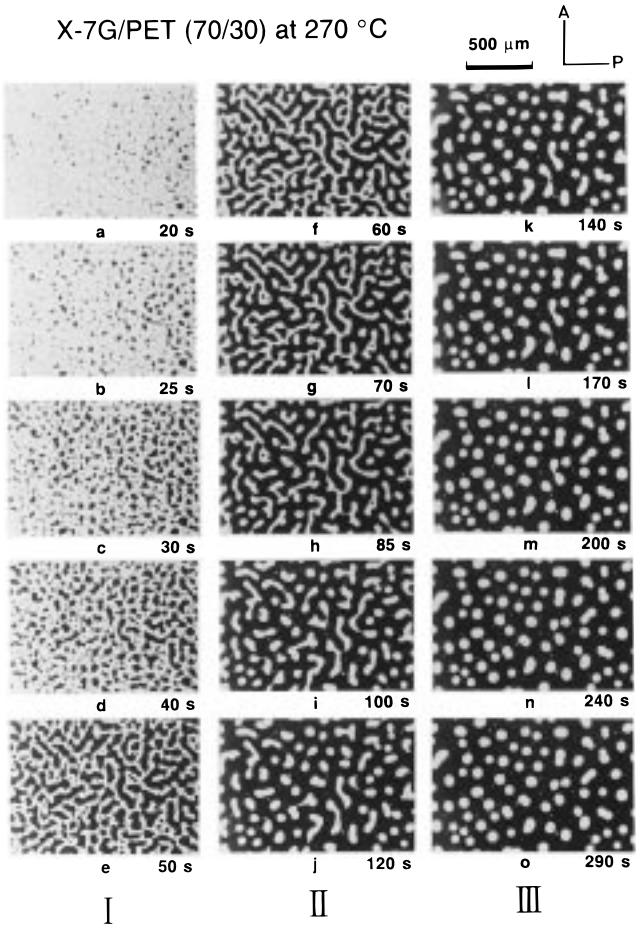

Figure 6. PLM micrographs of 70/30 showing the detailed growth of the domain structure at 270 °C for different annealing times. The delimitation of three regimes I−III is indicated in the figure according to the previously reported classification concepts for 50/50.[14] A and P designate the polarization directions of the analyzer and the polarizer.

large number of small isotropic droplets were first formed in the anisotropic matrix as mentioned above (see the image obtained at $t = 10$ s in Figure 1b). The rapid coalescence of the isotropic droplets led to the formation of larger isotropic domains, and their further growth resulted in the formation of the LC network ($t = 50$ s). It should be noted that the size of some of the isotropic domains at $t = 20$ s was already larger than the thickness of the film specimen. This implies that such isotropic domains were extended throughout the film thickness and the surface roughening of the film specimen was ready to occur. In fact, the dark area obviously increased with time, as shown by the images of "regime I" in Figure 6, indicating the protruding of the LC phase, due to the dewetting of the LC phase from the glass surface. This phenomenological explanation also accounts for the absence of regime I in the double logarithmic plot of Λ_m vs t for 70/30 in Figure 3. Therefore, "regime I" of 70/30 in Figure 6 should be classified to regime II.

Even at $t = 10$ s (Figure 1b) or 3 s (Figure 2) for 70/30, the isotropic phase of the dark droplets could be extending throughout the film thickness because if the LC phase had been overlapped on top of the isotropic phase, it should have appeared somewhat bright. If so, there should be many smaller droplets of the isotropic phase hidden in the Schlieren texture of the LC matrix in the PLM image of $t = 10$ s in Figure 1b, which might

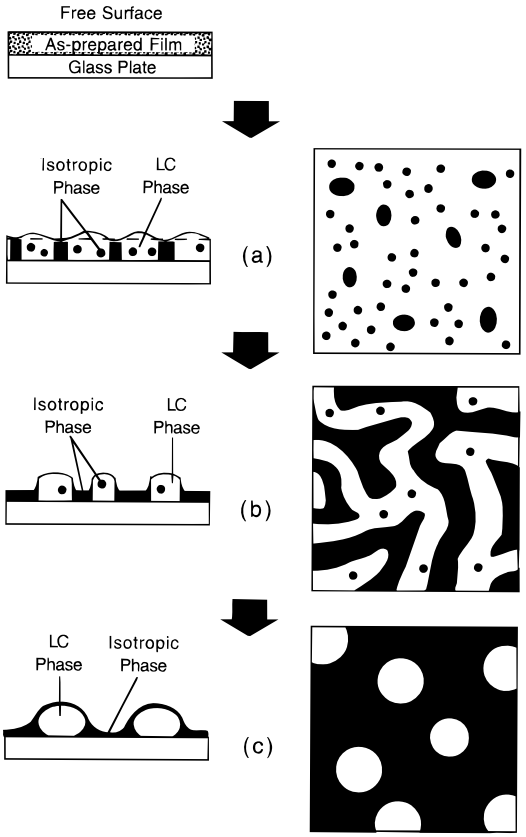

Figure 7. Schematic representation of the evolution of the phase-separated structure for 70/30: (left) side views; (right) top views.

be the reason that the distribution of the dark droplets is not uniform.

The pattern formation process for 70/30 is schematically illustrated in Figure 7: (a) Rapid coalescence of the isotropic droplets leads to the formation of large isotropic domains extending throughout the film thickness and the surface undulation starts to occur. (b) Further coalescence of the isotropic domains results in the formation of the LC network that protrudes from the isotropic matrix and contains the small isotropic droplets that are eventually driven out of the LC phase. (c) Disruption of the LC network results in the LC droplets in the isotropic matrix, which is essentially the same final structure as the one shown in Figure 5c. It has been shown that the surface of the LC droplets is covered with a thin layer of the isotropic phase.[14]

In Figure 8, the details of domain growth occurring in 70/30 observed at a high magnification are shown. Three kinds of mechanisms of domain growth were observed. Arrows A and B show the expelling of the isotropic droplets in the LC domains. The isotropic droplets were gradually expelled from the anisotropic domains as the time elapsed. Arrow C shows the diminishing (vaporization−condensation[17]) process of an isotropic droplet that was observed and discussed in our previous work on 50/50.[14] Arrow D demonstrates the disruption of a part of the anisotropic network. From $t = 45$ to 51 s, a part of the network became thinner and thinner, indicating that the LC molecules flowed from the thin part into the adjacent thicker parts. The flow tended to orient the LC molecules, thus the oriented part of the LC phase is all bright and defect free, as shown at $t = 51$ s. The disruption occurred not at the oriented part but at the regions near the thick parts of

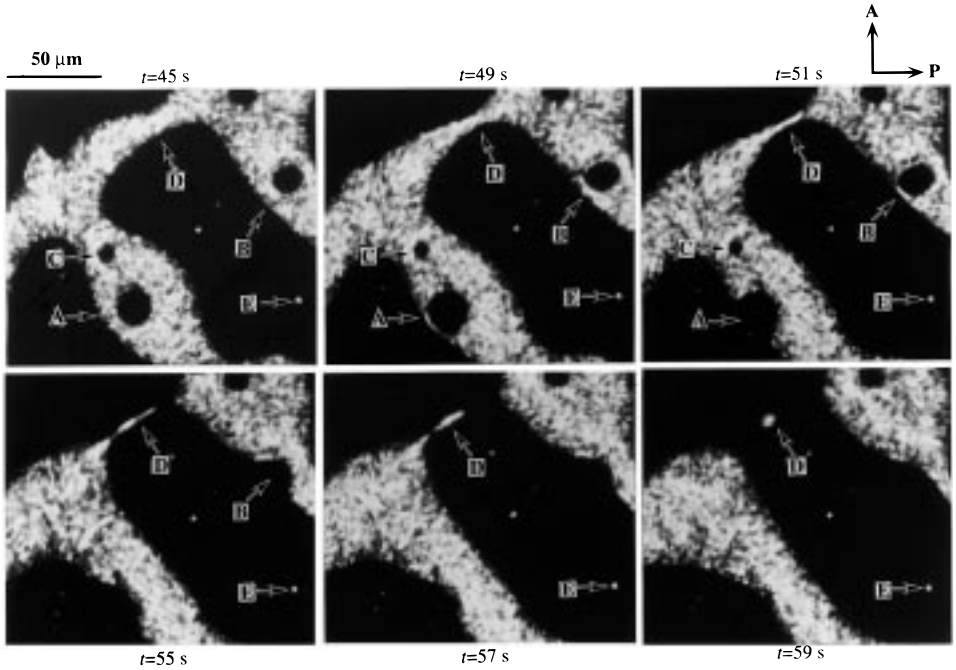

Figure 8. PLM micrographs of the film sample 70/30 obtained from the same area between $t = 45$ and 59 s during the isothermal annealing at 270 °C. The details of the specific mechanisms of the domain growth are marked by the arrows.

the network where the defects of the LC structure were probably existing, as shown in the images at $t = 55$ and 57 s. Thus, an isolated LC fragment was formed and it shrank into a small droplet, as shown in the image at $t = 59$ s. Many such small isolated LC droplets were observed as pointed out by arrow E in Figure 8.

It should be noted that all three mechanisms had similar time scales and were complete within 15 s. This implies that the origins of the three mechanisms are probably the same and controlled by the flow of the LC molecules. The diminishing process of an isotropic droplet was also observed and discussed in our previous work on 50/50[14] and attributed to a vaporization−condensation process.[17] Finally, the isotropic droplets formed in the early stage of the phase separation are not round but appear to have edges, as shown in Figure 2. This might be due to an elastic effect of LC matrix on the isotropic domains, further studies of which may be of worth as a future study.

E. Composition Dependence of the Final LC Droplet Size. The disruption of the LC network was the dominant mechanism leading to the growth of the domain structure in size in regimes I and II, although the different power laws were observed in the two regimes. This difference primarily resulted from the dewetting phenomenon in regime II, which also affects the final droplet size. A phenomenological explanation of the composition dependence of the final droplet size shown in Figure 4 is illustrated in Figure 9. For the mere spinodal decomposition of polymer mixtures, the final droplet size is determined by the percolation-cluster transition and subsequent spontaneous pinning and expected to increase as the composition approaches the critical one, as shown by the curve in Figure 9a. The size becomes infinity at the limit of the critical composition. In Figure 9a, the curve is shown only for the compositions with $\Phi_{X-7G} < 0.5$ because the dewetting is dominant for the compositions with $\Phi_{X-7G} > 0.5$. On the other hand, for a pure dewetting phenomenon the droplet size may be a monotonic increasing function

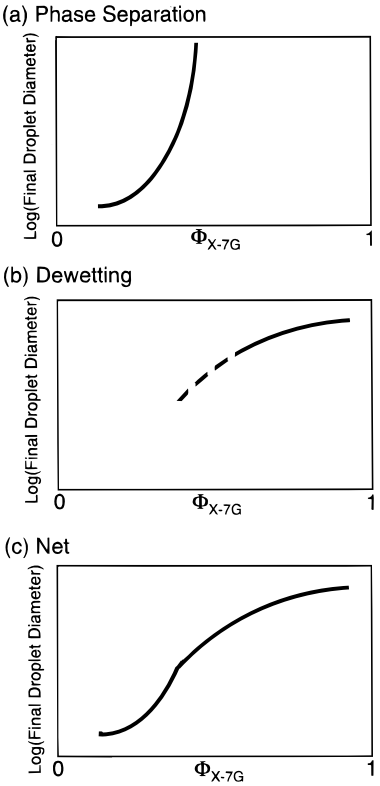

Figure 9. Schematic representation of the dependence of the average final droplet size on the composition of the mixture: (a) phase separation; (b) dewetting; (c) net.

of the LC content, as shown by the curve in Figure 9b, though its absolute value should be much larger than the spinodal decomposition case. The net curve synthesized from these two curves will have an S shape (Figure 9c) and qualitatively explains the composition dependence of the final droplet size in Figure 4, where the droplet size is considered to be controlled by the spinodal decomposition up to the composition of 40/60 and by the dewetting for the rest of the composition. It

should be noted that the droplet formation on the glass surface was observed even for pure X-7G.[18]

5. Conclusions

Composition dependence of the pattern formation processes on isothermal heat treatment (above the melting points) of the polymer mixtures consisting of a thermotropic liquid crystalline (LC) copolyester (X-7G) and poly(ethylene terephthalate) (PET) was investigated for the thin film specimens cast on a microscope cover glass by polarized light microscopy. The initial specimens were optically isotropic, homogeneous mixtures, and the final structures were optically anisotropic liquid-crystalline (LC) droplets rich in X-7G dispersed in the matrix of optically isotropic matrix rich in PET for all the compositions investigated. However, a variety of pattern formation processes were observed for the mixtures with different compositions. Two physical phenomena are responsible for the pattern formations: one is phase-separation by spinodal decomposition of the two component polymers, and the other is dewetting of the LC component (X-7G) against the glass surface.

For the mixtures with X-7G/PET ratios of 30/70 and 40/60, the structure with the LC droplets dispersed in the isotropic matrix was formed very quickly by phase separation and did not grow further, resulting in very small droplet sizes. For the mixtures with X-7G/PET ratios of 45/55, 50/50, and 60/40, three time regimes were observed for the pattern formation processes. A network structure of the LC phase formed first by spinodal decomposition (regime I), but dewetting of the LC phase against the glass surface caused the disruption of the LC network and the formation of the LC droplets (regime II) followed by the diffusion and coalescence of the droplets (regime III), resulting in much larger droplet sizes. In each regime, the time dependence of the average characteristic length Λ_m is scaled by a power law. For the mixtures with an X-7G/PET ratio of 70/30, the pattern formation process was quite different from that of the other mixtures. First, the isotropic droplets were formed in the LC matrix, followed by the formation of the LC network with the isotropic droplets inside, the disruption of the LC network and the formation and growth of the LC droplets. However, in terms of the time dependence of Λ_m only regimes II and III were observed, implying that dewetting is responsible for the entire process of the pattern formation.

Acknowledgment. This work has been supported by a Grant-in-Aid for Priority Areas, "Cooperative Phenomena in Complex Liquids" from the Ministry of Education, Science, and Culture, Japan (07236103), and by a scientific grant from Polyplastics Co. Ltd., Japan.

References and Notes

(1) Dutta, D.; Fruitwala, H.; Kohli, A.; Weiss, R. A. *Polym. Eng. Sci.* **1990**, *30*, 1005.
(2) Roetting, O.; Hinrichsen, G. *Adv. Polym. Technol.* **1994**, *13*, 57.
(3) Helminiak, T. E.; Arnold, F. E.; Benner, C. L. *Polym. Prepr. (Am. Chem. Soc., Div. Polym. Chem.)* **1975**, *16*, 659.
(4) Takayanagi, M.; Ogata, T. *J. Macromol. Sci. Phys. B* **1980**, *17*, 591.
(5) Hwang, W. F.; Wiff, D. R.; Benner, C. L. *J. Macromol. Sci. Phys. B* **1983**, *22*, 231.
(6) Wickliffe, S. M.; Farris, R. J.; Malone, M. F. *J. Appl. Polym. Sci.* **1987**, *34*, 931.
(7) Nehme, O. A.; Gabriel, C. A.; Farris, R. J.; Thomas, E. L.; Malone, M. F. *J. Appl. Polym. Sci.* **1988**, *35*, 1955.
(8) Siegmann, A.; Dagan, A.; Kenig, S. *Polymer* **1985**, *26*, 1325.
(9) Blizard, K. G.; Baird, D. G. *Polym. Eng. Sci.* **1987**, *27*, 653.
(10) Ko, C. U.; Wilkes, G. L. *J. Appl. Polym. Sci.* **1989**, *37*, 3063.
(11) Nobile, M. R.; Amendola, E.; Nicolais, Acierno, D.; Carfagna, C. *Polym. Eng. Sci.* **1989**, *29*, 244.
(12) Sukhadia, A. M.; Dong, D.; Baird, D. G. *Polym. Eng. Sci.* **1990**, *30*, 519.
(13) Nakai, A.; Shiwaku, T.; Wang, W.; Hasegawa, H.; Hashimoto, T. *Polymer* **1996**, *37*, 2259.
(14) Nakai, A.; Shiwaku, T.; Wang, W.; Hasegawa, H.; Hashimoto, T. *Macromolecules* **1996**, *29*, 5990.
(15) Wang, W.; Hashimoto, T. *J. Phys. Soc. Jpn.* **1996**, *65*, 3896 and the references therein.
(16) Nagaya, A.; Orihara, H.; Ishibashi, Y. *J. Phys. Soc. Jpn.* **1989**, *58*, 3600. This diffusion is driven by the interfacial tension and quite different from the Brownian diffusion for the case of 20/80 and 30/70.
(17) Lifshitz, I. M.; Slyozov, V. V. *Phys. Chem. Solids* **1961**, *19*, 35.
(18) Shiwaku, T.; Nakai, A.; Hasegawa, H.; Hashimoto, T. *Macromolecules* **1990**, *23*, 1590.

MA980070E